

# Measurement of the Time-Dependent $CP$ Asymmetry of Partially Reconstructed $B^0 \rightarrow D^{*+} D^{*-}$ Decays

J. P. Lees, V. Poireau, and V. Tisserand

*Laboratoire d'Annecy-le-Vieux de Physique des Particules (LAPP),  
Université de Savoie, CNRS/IN2P3, F-74941 Annecy-Le-Vieux, France*

J. Garra Tico and E. Grauges

*Universitat de Barcelona, Facultat de Física, Departament ECM, E-08028 Barcelona, Spain*

A. Palano<sup>ab</sup>

*INFN Sezione di Bari<sup>a</sup>; Dipartimento di Fisica, Università di Bari<sup>b</sup>, I-70126 Bari, Italy*

G. Eigen and B. Stugu

*University of Bergen, Institute of Physics, N-5007 Bergen, Norway*

D. N. Brown, L. T. Kerth, Yu. G. Kolomensky, and G. Lynch

*Lawrence Berkeley National Laboratory and University of California, Berkeley, California 94720, USA*

H. Koch and T. Schroeder

*Ruhr Universität Bochum, Institut für Experimentalphysik 1, D-44780 Bochum, Germany*

D. J. Asgeirsson, C. Hearty, T. S. Mattison, J. A. McKenna, and R. Y. So

*University of British Columbia, Vancouver, British Columbia, Canada V6T 1Z1*

A. Khan

*Brunel University, Uxbridge, Middlesex UB8 3PH, United Kingdom*

V. E. Blinov, A. R. Buzykaev, V. P. Druzhinin, V. B. Golubev, E. A. Kravchenko, A. P. Onuchin,

S. I. Serednyakov, Yu. I. Skovpen, E. P. Solodov, K. Yu. Todyshev, and A. N. Yushkov

*Budker Institute of Nuclear Physics, Novosibirsk 630090, Russia*

M. Bondioli, D. Kirkby, A. J. Lankford, and M. Mandelkern

*University of California at Irvine, Irvine, California 92697, USA*

H. Atmacan, J. W. Gary, F. Liu, O. Long, and G. M. Vitug

*University of California at Riverside, Riverside, California 92521, USA*

C. Campagnari, T. M. Hong, D. Kovalskyi, J. D. Richman, and C. A. West

*University of California at Santa Barbara, Santa Barbara, California 93106, USA*

A. M. Eisner, J. Kroseberg, W. S. Lockman, A. J. Martinez, B. A. Schumm, and A. Seiden

*University of California at Santa Cruz, Institute for Particle Physics, Santa Cruz, California 95064, USA*

D. S. Chao, C. H. Cheng, B. Echenard, K. T. Flood, D. G. Hitlin, P. Ongmongkolkul, F. C. Porter, and A. Y. Rakitin

*California Institute of Technology, Pasadena, California 91125, USA*

R. Andreassen, Z. Huard, B. T. Meadows, M. D. Sokoloff, and L. Sun

*University of Cincinnati, Cincinnati, Ohio 45221, USA*

P. C. Bloom, W. T. Ford, A. Gaz, U. Nauenberg, J. G. Smith, and S. R. Wagner

*University of Colorado, Boulder, Colorado 80309, USA*

R. Ayad\* and W. H. Toki

*Colorado State University, Fort Collins, Colorado 80523, USA*

B. Spaan

*Technische Universität Dortmund, Fakultät Physik, D-44221 Dortmund, Germany*

K. R. Schubert and R. Schwier  
*Technische Universität Dresden, Institut für Kern- und Teilchenphysik, D-01062 Dresden, Germany*

D. Bernard and M. Verderi  
*Laboratoire Leprince-Ringuet, Ecole Polytechnique, CNRS/IN2P3, F-91128 Palaiseau, France*

P. J. Clark and S. Playfer  
*University of Edinburgh, Edinburgh EH9 3JZ, United Kingdom*

D. Bettoni<sup>a</sup>, C. Bozzi<sup>a</sup>, R. Calabrese<sup>ab</sup>, G. Cibinetto<sup>ab</sup>, E. Fioravanti<sup>ab</sup>,  
 I. Garzia<sup>ab</sup>, E. Luppi<sup>ab</sup>, M. Menerato<sup>ab</sup>, L. Piemontese<sup>a</sup>, and V. Santoro<sup>a</sup>  
*INFN Sezione di Ferrara<sup>a</sup>; Dipartimento di Fisica, Università di Ferrara<sup>b</sup>, I-44100 Ferrara, Italy*

R. Baldini-Feroli, A. Calcaterra, R. de Sangro, G. Finocchiaro,  
 P. Patteri, I. M. Peruzzi,<sup>†</sup> M. Piccolo, M. Rama, and A. Zallo  
*INFN Laboratori Nazionali di Frascati, I-00044 Frascati, Italy*

R. Contri<sup>ab</sup>, E. Guido<sup>ab</sup>, M. Lo Vetere<sup>ab</sup>, M. R. Monge<sup>ab</sup>, S. Passaggio<sup>a</sup>, C. Patrignani<sup>ab</sup>, and E. Robutti<sup>a</sup>  
*INFN Sezione di Genova<sup>a</sup>; Dipartimento di Fisica, Università di Genova<sup>b</sup>, I-16146 Genova, Italy*

B. Bhuyan and V. Prasad  
*Indian Institute of Technology Guwahati, Guwahati, Assam, 781 039, India*

C. L. Lee and M. Morii  
*Harvard University, Cambridge, Massachusetts 02138, USA*

A. J. Edwards  
*Harvey Mudd College, Claremont, California 91711, USA*

A. Adametz and U. Uwer  
*Universität Heidelberg, Physikalisches Institut, Philosophenweg 12, D-69120 Heidelberg, Germany*

H. M. Lacker and T. Lueck  
*Humboldt-Universität zu Berlin, Institut für Physik, Newtonstr. 15, D-12489 Berlin, Germany*

P. D. Dauncey  
*Imperial College London, London, SW7 2AZ, United Kingdom*

U. Mallik  
*University of Iowa, Iowa City, Iowa 52242, USA*

C. Chen, J. Cochran, W. T. Meyer, S. Prell, and A. E. Rubin  
*Iowa State University, Ames, Iowa 50011-3160, USA*

A. V. Gritsan and Z. J. Guo  
*Johns Hopkins University, Baltimore, Maryland 21218, USA*

N. Arnaud, M. Davier, D. Derkach, G. Grosdidier, F. Le Diberder, A. M. Lutz,  
 B. Malaescu, P. Roudeau, M. H. Schune, A. Stocchi, and G. Wormser  
*Laboratoire de l'Accélérateur Linéaire, IN2P3/CNRS et Université Paris-Sud 11,  
 Centre Scientifique d'Orsay, B. P. 34, F-91898 Orsay Cedex, France*

D. J. Lange and D. M. Wright  
*Lawrence Livermore National Laboratory, Livermore, California 94550, USA*

C. A. Chavez, J. P. Coleman, J. R. Fry, E. Gabathuler, D. E. Hutchcroft, D. J. Payne, and C. Touramanis  
*University of Liverpool, Liverpool L69 7ZE, United Kingdom*

A. J. Bevan, F. Di Lodovico, R. Sacco, and M. Sigamani  
*Queen Mary, University of London, London, E1 4NS, United Kingdom*

G. Cowan  
*University of London, Royal Holloway and Bedford New College, Egham, Surrey TW20 0EX, United Kingdom*

D. N. Brown and C. L. Davis  
*University of Louisville, Louisville, Kentucky 40292, USA*

A. G. Denig, M. Fritsch, W. Gradl, K. Griessinger, A. Hafner, and E. Prencipe  
*Johannes Gutenberg-Universität Mainz, Institut für Kernphysik, D-55099 Mainz, Germany*

R. J. Barlow,<sup>‡</sup> G. Jackson, and G. D. Lafferty  
*University of Manchester, Manchester M13 9PL, United Kingdom*

E. Behn, R. Cenci, B. Hamilton, A. Jawahery, and D. A. Roberts  
*University of Maryland, College Park, Maryland 20742, USA*

C. Dallapiccola  
*University of Massachusetts, Amherst, Massachusetts 01003, USA*

R. Cowan, D. Dujmic, and G. Sciolla  
*Massachusetts Institute of Technology, Laboratory for Nuclear Science, Cambridge, Massachusetts 02139, USA*

R. Cheaib, D. Lindemann, P. M. Patel,<sup>§</sup> and S. H. Robertson  
*McGill University, Montréal, Québec, Canada H3A 2T8*

P. Biassoni<sup>ab</sup>, N. Neri<sup>a</sup>, F. Palombo<sup>ab</sup>, and S. Stracka<sup>ab</sup>  
*INFN Sezione di Milano<sup>a</sup>; Dipartimento di Fisica, Università di Milano<sup>b</sup>, I-20133 Milano, Italy*

L. Cremaldi, R. Godang,<sup>¶</sup> R. Kroeger, P. Sonnek, and D. J. Summers  
*University of Mississippi, University, Mississippi 38677, USA*

X. Nguyen, M. Simard, and P. Taras  
*Université de Montréal, Physique des Particules, Montréal, Québec, Canada H3C 3J7*

G. De Nardo<sup>ab</sup>, D. Monorchio<sup>ab</sup>, G. Onorato<sup>ab</sup>, and C. Sciacca<sup>ab</sup>  
*INFN Sezione di Napoli<sup>a</sup>; Dipartimento di Scienze Fisiche,  
 Università di Napoli Federico II<sup>b</sup>, I-80126 Napoli, Italy*

M. Martinelli and G. Raven  
*NIKHEF, National Institute for Nuclear Physics and High Energy Physics, NL-1009 DB Amsterdam, The Netherlands*

C. P. Jessop, J. M. LoSecco, and W. F. Wang  
*University of Notre Dame, Notre Dame, Indiana 46556, USA*

K. Honscheid and R. Kass  
*Ohio State University, Columbus, Ohio 43210, USA*

J. Brau, R. Frey, N. B. Sinev, D. Strom, and E. Torrence  
*University of Oregon, Eugene, Oregon 97403, USA*

E. Feltresi<sup>ab</sup>, N. Gagliardi<sup>ab</sup>, M. Margoni<sup>ab</sup>, M. Morandin<sup>a</sup>,  
 M. Posocco<sup>a</sup>, M. Rotondo<sup>a</sup>, G. Simi<sup>a</sup>, F. Simonetto<sup>ab</sup>, and R. Stroili<sup>ab</sup>  
*INFN Sezione di Padova<sup>a</sup>; Dipartimento di Fisica, Università di Padova<sup>b</sup>, I-35131 Padova, Italy*

S. Akar, E. Ben-Haim, M. Bomben, G. R. Bonneaud, H. Briand, G. Calderini,  
 J. Chauveau, O. Hamon, Ph. Leruste, G. Marchiori, J. Ocariz, and S. Sitt

*Laboratoire de Physique Nucléaire et de Hautes Energies,  
IN2P3/CNRS, Université Pierre et Marie Curie-Paris6,  
Université Denis Diderot-Paris7, F-75252 Paris, France*

M. Biasini<sup>ab</sup>, E. Manoni<sup>ab</sup>, S. Pacetti<sup>ab</sup>, and A. Rossi<sup>ab</sup>  
*INFN Sezione di Perugia<sup>a</sup>; Dipartimento di Fisica, Università di Perugia<sup>b</sup>, I-06100 Perugia, Italy*

C. Angelini<sup>ab</sup>, G. Batignani<sup>ab</sup>, S. Bettarini<sup>ab</sup>, M. Carpinelli<sup>ab,\*</sup>, G. Casarosa<sup>ab</sup>, A. Cervelli<sup>ab</sup>, F. Forti<sup>ab</sup>,  
M. A. Giorgi<sup>ab</sup>, A. Lusiani<sup>ac</sup>, B. Oberhof<sup>ab</sup>, E. Paoloni<sup>ab</sup>, A. Perez<sup>a</sup>, G. Rizzo<sup>ab</sup>, and J. J. Walsh<sup>a</sup>  
*INFN Sezione di Pisa<sup>a</sup>; Dipartimento di Fisica, Università di Pisa<sup>b</sup>; Scuola Normale Superiore di Pisa<sup>c</sup>, I-56127 Pisa, Italy*

D. Lopes Pegna, J. Olsen, A. J. S. Smith, and A. V. Telnov  
*Princeton University, Princeton, New Jersey 08544, USA*

F. Anulli<sup>a</sup>, R. Faccini<sup>ab</sup>, F. Ferrarotto<sup>a</sup>, F. Ferroni<sup>ab</sup>, M. Gaspero<sup>ab</sup>, L. Li Gioi<sup>a</sup>, M. A. Mazzoni<sup>a</sup>, and G. Piredda<sup>a</sup>  
*INFN Sezione di Roma<sup>a</sup>; Dipartimento di Fisica,  
Università di Roma La Sapienza<sup>b</sup>, I-00185 Roma, Italy*

C. Bünger, O. Grünberg, T. Hartmann, T. Leddig, H. Schröder,<sup>§</sup> C. Voss, and R. Waldi  
*Universität Rostock, D-18051 Rostock, Germany*

T. Adye, E. O. Olaiya, and F. F. Wilson  
*Rutherford Appleton Laboratory, Chilton, Didcot, Oxon, OX11 0QX, United Kingdom*

S. Emery, G. Hamel de Monchenault, G. Vasseur, and Ch. Yèche  
*CEA, Irfu, SPP, Centre de Saclay, F-91191 Gif-sur-Yvette, France*

D. Aston, D. J. Bard, R. Bartoldus, J. F. Benitez, C. Cartaro, M. R. Convery, J. Dorfan, G. P. Dubois-Felsmann,  
W. Dunwoodie, M. Ebert, R. C. Field, M. Franco Sevilla, B. G. Fulsom, A. M. Gabareen, M. T. Graham,  
P. Grenier, C. Hast, W. R. Innes, M. H. Kelsey, P. Kim, M. L. Kocian, D. W. G. S. Leith, P. Lewis, B. Lindquist,  
S. Luitz, V. Luth, H. L. Lynch, D. B. MacFarlane, D. R. Muller, H. Neal, S. Nelson, M. Perl, T. Pulliam,  
B. N. Ratcliff, A. Roodman, A. A. Salnikov, R. H. Schindler, A. Snyder, D. Su, M. K. Sullivan, J. Va'vra,  
A. P. Wagner, W. J. Wisniewski, M. Wittgen, D. H. Wright, H. W. Wulsin, C. C. Young, and V. Ziegler  
*SLAC National Accelerator Laboratory, Stanford, California 94309 USA*

W. Park, M. V. Purohit, R. M. White, and J. R. Wilson  
*University of South Carolina, Columbia, South Carolina 29208, USA*

A. Randle-Conde and S. J. Sekula  
*Southern Methodist University, Dallas, Texas 75275, USA*

M. Bellis, P. R. Burchat, T. S. Miyashita, and E. M. T. Puccio  
*Stanford University, Stanford, California 94305-4060, USA*

M. S. Alam and J. A. Ernst  
*State University of New York, Albany, New York 12222, USA*

R. Gorodeisky, N. Guttman, D. R. Peimer, and A. Soffer  
*Tel Aviv University, School of Physics and Astronomy, Tel Aviv, 69978, Israel*

P. Lund and S. M. Spanier  
*University of Tennessee, Knoxville, Tennessee 37996, USA*

J. L. Ritchie, A. M. Ruland, R. F. Schwitters, and B. C. Wray  
*University of Texas at Austin, Austin, Texas 78712, USA*

J. M. Izen and X. C. Lou  
*University of Texas at Dallas, Richardson, Texas 75083, USA*

F. Bianchi<sup>ab</sup>, D. Gamba<sup>ab</sup>, and S. Zambito<sup>ab</sup>  
*INFN Sezione di Torino<sup>a</sup>; Dipartimento di Fisica Sperimentale, Università di Torino<sup>b</sup>, I-10125 Torino, Italy*

L. Lanceri<sup>ab</sup> and L. Vitale<sup>ab</sup>  
*INFN Sezione di Trieste<sup>a</sup>; Dipartimento di Fisica, Università di Trieste<sup>b</sup>, I-34127 Trieste, Italy*

F. Martinez-Vidal and A. Oyanguren  
*IFIC, Universitat de Valencia-CSIC, E-46071 Valencia, Spain*

H. Ahmed, J. Albert, Sw. Banerjee, F. U. Bernlochner, H. H. F. Choi, G. J. King,  
 R. Kowalewski, M. J. Lewczuk, I. M. Nugent, J. M. Roney, R. J. Sobie, and N. Tasneem  
*University of Victoria, Victoria, British Columbia, Canada V8W 3P6*

T. J. Gershon, P. F. Harrison, and T. E. Latham  
*Department of Physics, University of Warwick, Coventry CV4 7AL, United Kingdom*

H. R. Band, S. Dasu, Y. Pan, R. Prepost, and S. L. Wu  
*University of Wisconsin, Madison, Wisconsin 53706, USA*  
 (Dated: 31 October, 2012)

We present a new measurement of the time-dependent  $CP$  asymmetry of  $B^0 \rightarrow D^{*+}D^{*-}$  decays using  $(471 \pm 5)$  million  $B\bar{B}$  pairs collected with the *BABAR* detector at the PEP-II  $B$  Factory at the SLAC National Accelerator Laboratory. Using the technique of partial reconstruction, we measure the time-dependent  $CP$  asymmetry parameters  $S = -0.34 \pm 0.12 \pm 0.05$  and  $C = +0.15 \pm 0.09 \pm 0.04$ . Using the value for the  $CP$ -odd fraction  $R_{\perp} = 0.158 \pm 0.028 \pm 0.006$ , previously measured by *BABAR* with fully reconstructed  $B^0 \rightarrow D^{*+}D^{*-}$  events, we extract the  $CP$ -even components  $S_+ = -0.49 \pm 0.18 \pm 0.07 \pm 0.04$  and  $C_+ = +0.15 \pm 0.09 \pm 0.04$ . In each case, the first uncertainty is statistical and the second is systematic; the third uncertainty on  $S_+$  is the contribution from the uncertainty on  $R_{\perp}$ . The measured value of the  $CP$ -even component  $S_+$  is consistent with the value of  $\sin 2\beta$  measured in  $b \rightarrow (c\bar{c})s$  transitions, and with the Standard Model expectation of small penguin contributions.

PACS numbers: 13.25.Hw, 12.15.Hh, 11.30.Er

(Submitted to Phys. Rev. D)

## I. INTRODUCTION

In the Standard Model (SM),  $CP$  violation arises from an irreducible complex phase in the  $3 \times 3$  quark mixing matrix  $V$  known as the Cabibbo-Kobayashi-Maskawa (CKM) matrix [1, 2]. Unitarity of the CKM matrix requires that the relation  $V_{ud}V_{ub}^* + V_{cd}V_{cb}^* + V_{td}V_{tb}^* = 0$ , which defines the unitarity triangle, be satisfied. The aim of the  $B$  Factories is to test the unitarity of the CKM matrix by the precise measurement of the angles and sides of the above triangle, whose nonvanishing area indicates violation of  $CP$  symmetry.

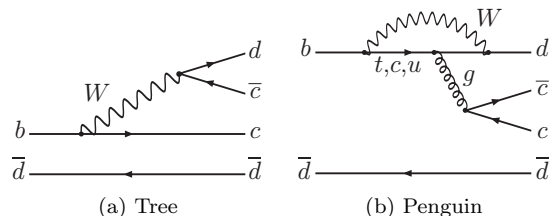


FIG. 1: Leading and sub-leading order Feynman graphs for the  $\bar{B}^0 \rightarrow D^{(*)+}D^{(*)-}$  decays.

Both the *BABAR* and Belle collaborations have measured the  $CP$  parameter  $\sin 2\beta$ , where the angle  $\beta$  is defined as  $\beta \equiv \arg[-V_{cd}V_{cb}^*/V_{td}V_{tb}^*]$ . The most accurate measurements of  $\sin 2\beta$  [3–5] use the  $b \rightarrow (c\bar{c})s$  transition, in which  $B^0$ 's decay to charmonium final states. Measurement of  $b \rightarrow c\bar{c}d$  transitions such as  $B^0 \rightarrow D^{(*)+}D^{(*)-}$  should yield the same value of  $\sin 2\beta$  to the extent that the contributions from penguin processes may be neglected.

The leading and sub-leading order Feynman diagrams contributing to  $B^0 \rightarrow D^{(*)+}D^{(*)-}$  decays are shown in Fig. 1. The effect of neglecting the penguin amplitude has been estimated in models based on factorization and heavy quark symmetry, and the corrections are found to be a few percent [6, 7]. Loops involving non-SM particles

\*Now at the University of Tabuk, Tabuk 71491, Saudi Arabia

†Also with Università di Perugia, Dipartimento di Fisica, Perugia, Italy

‡Now at the University of Huddersfield, Huddersfield HD1 3DH, UK

§Deceased

¶Now at University of South Alabama, Mobile, Alabama 36688, USA

\*\*Also with Università di Sassari, Sassari, Italy

(for example, charged Higgs or SUSY particles) could increase the contribution from penguin diagrams and introduce additional phases.

In  $\Upsilon(4S) \rightarrow B^0 \bar{B}^0$  events the time-dependent decay rate for  $B^0 \rightarrow D^{*+} D^{*-}$  is given by

$$P_\eta^{S_{\text{tag}}}(\Delta t) = \frac{e^{-|\Delta t|/\tau_b}}{4\tau_b} \cdot [1 + S_{\text{tag}} S_\eta \sin(\Delta m_d \Delta t) + S_{\text{tag}} C \cos(\Delta m_d \Delta t)], \quad (1)$$

where  $\tau_b$  is the  $B^0$  lifetime averaged over the two mass eigenstates,  $\Delta m_d$  is the  $B^0 \bar{B}^0$  mixing frequency, and  $\Delta t$  is the time interval between the  $B^0 \rightarrow D^{*+} D^{*-}$  decay ( $B_{\text{rec}}$ ) and the decay of the other  $B$  ( $B_{\text{tag}}$ ) in the event. The parameter  $S_{\text{tag}} = +1$  ( $-1$ ) in Eq. (1) indicates the flavor of the  $B_{\text{tag}}$  as a  $B^0$  ( $\bar{B}^0$ ), while  $\eta = \pm 1$  indicates the  $CP$  eigenvalue of the  $B^0 \rightarrow D^{*+} D^{*-}$  final state. The parameters  $C$  and  $S_\eta$  are given by

$$C = \frac{1 - |\lambda|^2}{1 + |\lambda|^2}; \quad S_\eta = -\eta \frac{2\Im m(\lambda)}{1 + |\lambda|^2}; \quad \lambda = \frac{q}{p} \frac{\bar{A}}{A}, \quad (2)$$

where  $A$  ( $\bar{A}$ ) is the matrix element of the  $B^0$  ( $\bar{B}^0$ ) decay and  $p$  and  $q$  are the coefficients appearing in the expression of the physical mass eigenstates  $B_L$ ,  $B_H$  in terms of the flavour eigenstates  $B$ ,  $\bar{B}$ :

$$\begin{aligned} |B_L\rangle &= p|B\rangle + q|\bar{B}\rangle \\ |B_H\rangle &= p|B\rangle - q|\bar{B}\rangle. \end{aligned}$$

Since the  $B^0 \rightarrow D^{*+} D^{*-}$  is the decay of a scalar to two vector mesons, the final state is a mixture of  $CP$  eigenstates. The  $CP$ -odd and  $CP$ -even fractions have been previously measured from the angular analysis of completely reconstructed events [8, 9].

A large deviation of the measured parameter  $S_\eta$  in Eq. 2 from the value of  $\sin 2\beta$  measured in  $b \rightarrow (c\bar{c})s$  transitions or a non-zero value of direct  $CP$  violation [10–12] would be strong evidence of new physics.

Both the *BABAR* [8] and Belle [9] collaborations have studied the  $CP$  asymmetries of  $B^0 \rightarrow D^{*+} D^{*-}$  decays using fully reconstructed events. In this article we report a new measurement based on the technique of partial reconstruction, which allows us to gain a factor of  $\simeq 5$  in the number of selected signal events with respect to the most recent *BABAR* full reconstruction analysis in [8]. This result is complementary to the latter measurement, because the statistics used are largely independent of each other.

## II. THE *BABAR* DETECTOR AND DATASET

The data sample used in this analysis has been collected with the *BABAR* detector [13] operating at the PEP-II asymmetric-energy  $B$  Factory located at the SLAC National Accelerator Laboratory. We have analyzed the full *BABAR* data set collected at the  $\Upsilon(4S)$  mass peak,

$\sqrt{s} = 10.58$  GeV, corresponding to an integrated luminosity of  $429.0 \text{ fb}^{-1}$ . In addition, we have used  $44.8 \text{ fb}^{-1}$  of data taken off-resonance to evaluate the background from events  $e^+e^- \rightarrow q\bar{q}$ , where  $q$  represents a  $u, d, s$  or  $c$  quark (“continuum”). To study backgrounds and validate the analysis procedure, we use a *GEANT4*-based [14] Monte Carlo (MC) simulation in which coherent  $B\bar{B}$  production is simulated using the package *EvtGen* [15].

The asymmetric energies of the PEP-II beams are an ideal environment to study time-dependent  $CP$  phenomena in the  $B^0 \bar{B}^0$  system. The boost of the  $\Upsilon(4S)$  in the laboratory frame by  $\beta\gamma = 0.56$  increases the separation between the vertices of the two  $B$  meson daughters, allowing their precise measurement.

The *BABAR* detector is described in detail in Ref. [13]. We give here only a brief description of the main components and their use in this analysis. Tracking is provided by a five-layer silicon vertex detector (SVT) and a drift chamber (DCH). The SVT provides precise position measurements close to the interaction region that are used in vertex reconstruction and low-momentum track reconstruction. The DCH provides excellent momentum measurement of charged particles.

Particle identification (PID) of kaons and pions is obtained from ionization losses in the SVT and DCH and from measurements of photons produced in a ring-imaging Cherenkov light detector (DIRC). A CsI(Tl) crystal-based electromagnetic calorimeter (EMC) enables measurement of photon energies and electron identification. These systems all operate inside a 1.5 T superconducting solenoid, whose iron flux return is instrumented for muon detection, initially with resistive plate chambers and more recently with limited streamer tubes [16].

## III. ANALYSIS METHOD

### A. Partial Reconstruction

In the partial reconstruction of a  $B^0 \rightarrow D^{*+} D^{*-}$  candidate, we reconstruct fully only one of the two  $D^{*\pm}$  mesons in the decay chain  $D^* \rightarrow D^0 \pi$  [17], by identifying  $D^0$  candidates in one of four final states:  $K\pi$ ,  $K\pi\pi^0$ ,  $K\pi\pi\pi$ ,  $K_S^0\pi\pi$ . The vertexing algorithm fits the two-step decay tree simultaneously, correctly calculating correlations among all candidates. In the first three  $D^0$  decay modes, assumed to represent Cabibbo-favored decays, charged kaon tracks are selected using PID information from the DIRC, SVT and DCH. In the last decay mode,  $K_S^0$  candidates are selected by constraining pairs of oppositely charged tracks to a common vertex.

Since the kinetic energy available in the decay  $D^* \rightarrow D^0 \pi$  is small, we combine one reconstructed  $D^{*\pm}$  with an oppositely charged low-momentum pion, assumed to originate from the decay of the unreconstructed  $D^{*\mp}$ , and evaluate the mass  $m_{\text{rec}}$  of the recoiling  $D^0$  meson by using the momenta of the two particles. For signal events  $m_{\text{rec}}$  peaks at the nominal  $D^0$  mass [18] with an r.m.s. width

of about  $3 \text{ MeV}/c^2$ , while for background events no such peak is visible. Thus,  $m_{\text{rec}}$  is the primary variable to discriminate signal from background. The calculation of  $m_{\text{rec}}$  proceeds as follows (refer to Fig. 2 for definitions of the various momenta and angles that we use).

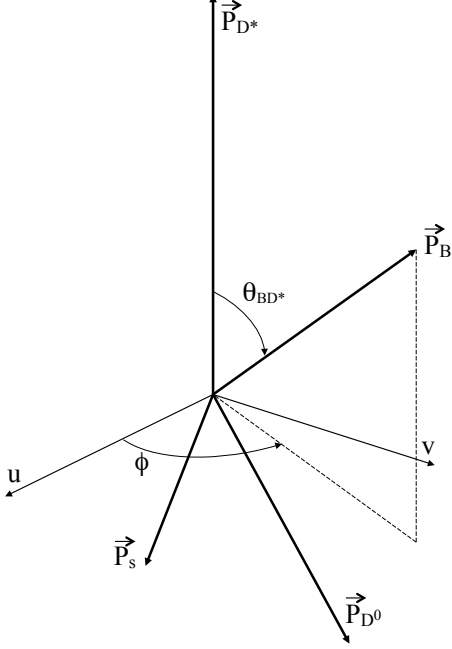


FIG. 2: Momenta and angles in the  $\Upsilon(4S)$  center of mass frame used in partial reconstruction. The orthogonal axes  $u$  and  $v$  are normal to the momentum  $\vec{p}_{D^*}$  of the reconstructed  $D^*$ , and  $u$  lies in the plane defined by the momenta of the  $D^*$  and slow pion,  $\vec{p}_{D^*}$  and  $\vec{p}_s$ . The angle  $\phi$  is measured in the  $u-v$  plane.

The cosine of the angle between the momenta in the  $\Upsilon(4S)$  center of mass (CM) frame of the  $B$  and the reconstructed  $D^*$  is readily computed:

$$\cos \theta_{BD^*} = \frac{-M_{B^0}^2 + E_{\text{CM}} E_{D^*}}{2p_B |\vec{p}_{D^*}|}, \quad (3)$$

where all particle masses are set to their nominal values [18],  $E_{D^*}$  and  $\vec{p}_{D^*}$  are the measured energy and momentum of the reconstructed  $D^*$  in the  $\Upsilon(4S)$  CM frame,  $E_{\text{CM}}/2$  is the energy of each beam in the CM frame, and  $p_B = \sqrt{E_{\text{CM}}^2/4 - M_{B^0}^2}$  is the  $B$ -meson CM momentum. Events are required to be in the physical region  $|\cos \theta_{BD^*}| < 1$ .

Given  $\cos \theta_{BD^*}$  and the measured momenta of the  $D^*$  and oppositely charged low-momentum pion,  $\pi_s$ , the  $B$  four-momentum can be calculated up to an unknown azimuthal angle  $\phi$  around  $\vec{p}_{D^*}$ . For any chosen value

of  $\phi$ , conservation laws determine the unreconstructed  $D^0$  four-momentum  $q_D(\phi)$ , and one can thus compute the corresponding  $\phi$ -dependent invariant mass  $m(\phi) \equiv \sqrt{|q_D(\phi)|^2}$ . The value of  $\phi$  is not constrained by kinematics and may be chosen arbitrarily, to the extent that the shape of the resulting  $m(\phi)$  distribution may still be described by the type of functions used in our fits. We have chosen the value for which  $\cos \phi = 0.62$ , which is the median of the corresponding Monte Carlo distribution for signal events obtained using generated momenta, and define the recoiling  $D^0$  mass  $m_{\text{rec}} \equiv m(\cos \phi = 0.62)$ . We use the same convention to obtain the direction of the unreconstructed  $D^0$  meson.

## B. Backgrounds and Event Selection

Backgrounds to the  $B^0 \rightarrow D^{*+} D^{*-}$  process include the following:

- Combinatorial  $B\bar{B}$  background, defined as decays other than  $B^0 \rightarrow D^{*+} D^{*-}$ , for which the  $m_{\text{rec}}$  distribution is approximately flat.
- Peaking  $B\bar{B}$  background, defined as decays other than  $B^0 \rightarrow D^{*+} D^{*-}$ , in which the  $m_{\text{rec}}$  distribution peaks in the signal region. It will be shown later that the contribution from this background is negligible.
- Background from non- $b\bar{b}$  events.

Combinatorial  $B\bar{B}$  background events are reduced by the following requirements: For the  $K_s^0 \pi \pi$  mode, we require the invariant mass of the pion pair to be within  $25 \text{ MeV}/c^2$  of the  $K_s^0$  mass [18]. The corresponding vertex must be separated by more than  $3 \text{ mm}$  from the beam axis. For the  $K \pi \pi^0$  mode,  $\pi^0$  candidates are formed from pairs of photons detected in the EMC, with energies greater than  $40 \text{ MeV}$ , for which the invariant mass differs by less than  $20 \text{ MeV}/c^2$  from the nominal  $\pi^0$  mass [18]. The reconstructed  $D^0$  mass must be equal to the nominal one [18] within 2 or 2.5 standard deviations, depending on the  $D^0$  reconstruction mode. The momenta in the  $\Upsilon(4S)$  CM frame of the reconstructed  $D^*$  and  $\pi_s$  from the missing  $D^0$  must be, respectively, in the range  $1.3\text{--}2.1 \text{ GeV}/c$  and smaller than  $0.6 \text{ GeV}/c$ . The difference  $\Delta M = |M_{D^*} - M_{D^0} - M_\pi|$  must be equal to the nominal [18] value within 1 or  $1.5 \text{ MeV}/c^2$ , according to the presence or absence of DCH hits in the pion track appearing in the reconstructed decay  $D^* \rightarrow D^0 \pi$ . The probability of the vertex fits must be greater than  $10^{-2}$ , for both the  $D^0$  and the  $D^*$  reconstruction.

The requirement on the  $D^0$  vertex fit probability introduces a small but measurable bias toward lower values of the  $B$  lifetime. Due to partial reconstruction, the tracks used to make the  $D^0$  vertex may originate from the same or different  $B$  mesons. In the latter case, since not all tracks are from the same point in space, the  $\chi^2$  of the

vertex fit tends to be bigger. This effect worsens with increasing distance between the two  $B$  decay vertices, causing vertices further apart to be rejected more frequently. We have verified this on signal Monte Carlo events, for which we have measured a lifetime lower than the generated value. Consequently, for the signal  $\Delta t$  probability distribution functions (PDF's) we use the value of  $\tau_b$  fitted to signal Monte Carlo.

In events passing this selection we find more than one candidate decay chain in about 25% of the cases, usually differing only in the slow pion  $\pi_s$ , but sometimes in the components of the reconstructed  $D^*$ . When this happens, we choose one candidate chain, based respectively on the largest number of DCH hits in the  $\pi_s$ , or according to a  $\chi^2$  based on the reconstructed  $D^0$  mass and  $\Delta M$  quantity above. For signal Monte Carlo, the probability for this candidate chain to be the correct one is 0.95.

The main suppression of continuum background is obtained by requiring that the ratio  $R_2$  of the 2<sup>nd</sup> to the 0<sup>th</sup> Fox-Wolfram moment [19], computed using all charged particles and EMC clusters not matched to tracks, be less than 0.3.

### C. Fisher Discriminant

To further reduce continuum background, we combine several event-shape variables into a Fisher discriminant [20]  $F$ . Discriminating power originates from the observation that  $q\bar{q}$  events tend to be jet-like, whereas  $B\bar{B}$  events have a more spherical energy distribution. Rather than applying requirements on  $F$ , we use the corresponding distribution in the fits described in Sec. III E

Our Fisher discriminant is a linear combination of variables chosen, according to Monte Carlo studies, to maximize the separation between  $B\bar{B}$  and continuum events. The first nine variables describe the energy flow inside nine concentric cones centered around the direction of the reconstructed  $D^{*\pm}$ . In addition, we use the momenta of the charged and the neutral particle closest to the cone axis, the polar angles in the CM of the reconstructed  $D^*$  momentum and the thrust axis  $T$  for charged tracks in the  $B_{\text{tag}}$  vertex (see next paragraph), the angle between the reconstructed  $D^*$  momentum and  $T$ , and the sum  $S = \sum_i p_i \times P_2(\cos \theta_i)$  over the  $B_{\text{tag}}$  charged tracks, in which  $p_i$  is momentum,  $P_2$  is the 2<sup>nd</sup> Legendre polynomial of argument  $\cos \theta_i$ , and  $\theta_i$  is the angle between track  $i$  at the origin and  $T$ .

### D. Flavor Tagging and Decay Time Measurement

For this analysis, two measurements are needed: the difference  $\Delta t$  between the proper decay times of the partially reconstructed  $B$  meson and the other  $B$  meson in the event, and the flavor of the latter.

The flavor tagging algorithm is based on tracks identified as electrons, muons or kaons. The electron and

muon tags contribute equally to the total sample and, since these events are kinematically almost indistinguishable and have very similar effective tagging efficiency, we treat them as one homogeneous “lepton” sample.

The tagging tracks must be chosen among those not used in  $B_{\text{rec}}$  reconstruction and must originate from within 4 mm (3 cm) of the interaction point in the transverse (longitudinal) view. The momentum of the lepton candidates is required to be greater than 1.1 GeV/c in order to reject most leptons from charmed meson decays. If one or more lepton candidates are qualified, the tag flavor is assigned based on the charge of the lepton with the highest center-of-mass momentum. If two or more qualified kaons are present, the event is used only if the flavor is unambiguous. If both a lepton and a kaon tag are available, the lepton tag is used.

The time difference  $\Delta t$  is calculated using  $\Delta t = \Delta z / \gamma \beta c$ , where  $\Delta z = z_{\text{rec}} - z_{\text{tag}}$  is the difference between the  $z$ -coordinates of the partially reconstructed  $B_{\text{rec}}$  and  $B_{\text{tag}}$  vertices and the boost parameters are calculated using the measured beam energies. The uncertainty  $\sigma_{\Delta t}$  on  $\Delta t$  is calculated from the results of the  $z_{\text{rec}}$  and  $z_{\text{tag}}$  vertex fits. We require  $|\Delta t| < 20$  ps and  $\sigma_{\Delta t} < 2.5$  ps.

We define the  $B_{\text{rec}}$  vertex as the decay point of the fully reconstructed  $D^{*\pm}$ . The  $\pi_s$  track from the other  $D^{*\pm}$  is not used, since it undergoes significant multiple Coulomb scattering and hence does not improve the  $z_{\text{rec}}$  measurement resolution.

The  $B_{\text{tag}}$  vertex reconstruction depends on the tagging category. For kaon-tagged events, we obtain  $z_{\text{tag}}$  from a beam spot constrained vertex fit of all charged tracks in the event, excluding those from the  $B_{\text{rec}}$  meson, and excluding also tracks within 1 rad of the unreconstructed  $D^0$  momentum in the CM frame, which presumably originate from the  $D^0$  decay. We require the probability of this fit to be greater than  $10^{-2}$ . For lepton-tagged events, we use the lepton track parameters and errors, and the measured beam spot position and size in the plane perpendicular to the beams (the  $x$ - $y$  plane). We find the position of the point in space for which the sum of the  $\chi^2$  contributions from the lepton track and the beam spot is minimum. The  $z$  coordinate of this point is taken as  $z_{\text{tag}}$ .

The beam spot is measured on a run-by-run basis using 2-prong events (Bhabha and  $\mu^+\mu^-$ ), and has an r.m.s. size of approximately 120  $\mu\text{m}$  in the horizontal dimension ( $x$ ), 5  $\mu\text{m}$  in the vertical dimension ( $y$ ), and 8.5 mm along the beam direction ( $z$ ). The average  $B$  meson flight distance in the  $x$ - $y$  plane is 30  $\mu\text{m}$ . To account for the  $B$  flight distance in the beam spot constrained vertex fit, 30  $\mu\text{m}$  are added in quadrature to the effective  $x$  and  $y$  sizes.

### E. Probability Distribution Functions

We use two PDF's,  $P_{\text{on}}$  for on-resonance, and  $P_{\text{off}}$  for off-resonance data. The former depends on the variables



$m_{\text{rec}}$ ,  $F$ ,  $\Delta t$ ,  $\sigma_{\Delta t}$ ,  $S_{\text{tag}}$ , and is given by the sum of the PDF's for the different event types described above:

$$P_{\text{on}} = f_{B\bar{B}} [f_{\text{sig}} P_{\text{sig}} + (1 - f_{\text{sig}}) P_{\text{comb}}] + (1 - f_{B\bar{B}}) P_{q\bar{q}}(4)$$

where  $P_{\text{sig}}$ ,  $P_{\text{comb}}$ , and  $P_{q\bar{q}}$  are respectively the PDF's for signal events, for combinatorial background from  $B\bar{B}$ , and for continuum. Moreover,  $f_{B\bar{B}}$  is the fraction of  $B\bar{B}$  events in our sample, and  $f_{\text{sig}}$  is the fraction of signal events in  $B\bar{B}$  events. The PDF for off-resonance data,  $P_{\text{off}}$ , is reduced to just one component,  $P_{q\bar{q}}$ , as the off-peak sample contains only continuum events.

According to Monte Carlo, the distributions of  $B^0\bar{B}^0$  and  $B^+B^-$  combinatorial background events are very similar and can be described well by the same PDF.

We do not consider the fraction of  $B\bar{B}$  events a free parameter, but fix it to  $f_{B\bar{B}} = 1 - f_{q\bar{q}}$ , where  $f_{q\bar{q}}$  is the fraction of continuum events in the on-peak sample and is defined by

$$f_{q\bar{q}} = \frac{N_{\text{off-peak}}}{N_{\text{on-peak}}} \frac{\mathcal{L}_{\text{on-peak}}}{\mathcal{L}_{\text{off-peak}}}, \quad (5)$$

where  $N$ 's are the number of events left by our selection in the on- and off-peak samples and  $\mathcal{L}$ 's are the integrated on- and off-peak luminosities.

Each of the  $P_i$  ( $i = \text{sig}, \text{comb}, q\bar{q}$ ) can be expressed as the product of three one dimensional PDF's:

$$P_i(m_{\text{rec}}, F, \Delta t, \sigma_{\Delta t}, S_{\text{tag}}) = \mathcal{M}_i(m_{\text{rec}}) \mathcal{F}_i(F) T'_i(\Delta t, \sigma_{\Delta t}, S_{\text{tag}}), \quad (6)$$

that are the probability distributions of the recoil  $D^0$  mass  $\mathcal{M}_i(m_{\text{rec}})$ , the Fisher discriminant function  $\mathcal{F}_i(F)$ , and the decay time difference function  $T'_i(\Delta t, \sigma_{\Delta t}, S_{\text{tag}})$ . This follows from extensive Monte Carlo studies showing that the correlations among these variables are negligible.

### 1. $\mathcal{M}(m_{\text{rec}})$ and $\mathcal{F}(F)$ PDF's

The  $m_{\text{rec}}$  distribution of all sample components can be well modelled in the lower region of the spectrum with a so called "Argus function" [21]:

$$\mathcal{A}(m_{\text{rec}}) = m_{\text{rec}} \sqrt{1 - (m_{\text{rec}}/m_{\text{ep}})^2} \cdot e^{c \cdot m_{\text{rec}}/m_{\text{ep}}}, \quad (7)$$

where  $m_{\text{ep}}$  is the kinematic endpoint ( $m_{\text{rec}} \leq m_{\text{ep}}$ ) and  $c$  is a free parameter describing the slope. This function alone, however, is not sufficient to account for the abrupt fall of the  $m_{\text{rec}}$  spectrum near the kinematic endpoint. For the signal sample we model this shoulder with an asymmetric error function with widths  $\sigma_l$  and  $\sigma_r$ , tapered off at low  $m_{\text{rec}}$  by an exponential factor with decay constant  $a$ :

$$\mathcal{E}(m_{\text{rec}}) = \begin{cases} e^{m_{\text{rec}}/a} [1 - \text{erf}(m_{\text{rec}} - m_{\text{ep}})/(\sqrt{2}\sigma_l)], & m_{\text{rec}} < m_{\text{ep}} \\ e^{m_{\text{rec}}/a} [1 - \text{erf}(m_{\text{rec}} - m_{\text{ep}})/(\sqrt{2}\sigma_r)], & m_{\text{rec}} > m_{\text{ep}}. \end{cases}$$

Thus, we describe the signal  $m_{\text{rec}}$  distribution with a combination of three functions: a Gaussian  $G$  having average  $m_G$  and standard deviation  $\sigma_G$  for the well reconstructed peaking component; an Argus function, mainly for events in which the right  $D^*$  is combined with a low-momentum pion from another decay chain; and the  $\mathcal{E}$  function:

$$\begin{aligned} \mathcal{M}_{\text{sig}}(m_{\text{rec}}) = & f_{\text{sig}}^A \cdot \mathcal{A}(m_{\text{rec}}) + \\ & + (1 - f_{\text{sig}}^A) \cdot [f^G \cdot G(m_{\text{rec}}) \\ & + (1 - f^G) \cdot \mathcal{E}(m_{\text{rec}})]. \end{aligned} \quad (8)$$

In Eq. 8  $f_{\text{sig}}^A$  is the fraction of events described by the Argus component and  $f^G$  is the fraction of events in the Gaussian peak relative to the non-Argus component.

For the background, both combinatorial and continuum, we set the fraction of the Gaussian component to zero, and model the distribution at the endpoint with a simple error function of width  $\sigma$ . However, for the case of combinatorial background in kaon-tagged events, we find that two different Argus components ( $\mathcal{A}_1$  and  $\mathcal{A}_2$ ) are needed to correctly describe the entire reconstructed mass spectrum. We thus define two PDF's according to:

$$\begin{aligned} \mathcal{M}_{\text{comb}}(m_{\text{rec}}) = & f_{\text{comb}}^{\text{erf}} \cdot \text{erf}(m_{\text{rec}} - m_{\text{ep}}; \sigma_{\text{comb}}) + \\ & + (1 - f_{\text{comb}}^{\text{erf}}) \cdot [f_{\text{comb}}^{\mathcal{A}_1} \cdot \mathcal{A}_1(m_{\text{rec}}) + \\ & + (1 - f_{\text{comb}}^{\mathcal{A}_1}) \cdot \mathcal{A}_2(m_{\text{rec}})], \end{aligned} \quad (9)$$

$$\mathcal{M}_{q\bar{q}}(m_{\text{rec}}) = f_{q\bar{q}}^{\text{erf}} \cdot \text{erf}(m_{\text{rec}} - m_{\text{ep}}; \sigma_{q\bar{q}}) + (1 - f_{q\bar{q}}^{\text{erf}}) \cdot \mathcal{A}_1(m_{\text{rec}}). \quad (10)$$

The parameter  $m_{\text{ep}}$  represents simultaneously the two Argus endpoints and the error function inflection point.

The Fisher discriminant PDF  $\mathcal{F}_i$  is parameterized by two Gaussian functions for each event type  $i = (B\bar{B}, q\bar{q})$ , having standard deviations  $\sigma_i^L$  and  $\sigma_i^R$ , and common mean  $\mu_i$ :

$$\mathcal{F}_i(F) \propto \begin{cases} \exp[-(F - \mu_i)^2/2(\sigma_i^L)^2] & F < \mu_i \\ \exp[-(F - \mu_i)^2/2(\sigma_i^R)^2] & F > \mu_i. \end{cases} \quad (11)$$

Since the Fisher variable is designed to discriminate between  $q\bar{q}$  and  $B\bar{B}$  events, we expect the Fisher discriminant for signal events to be indistinguishable from that of  $B\bar{B}$  combinatorial events. We have verified this expectation with Monte Carlo studies, and thus use the same Fisher discriminant to describe both event types.

### 2. $\Delta t$ PDF's

The  $\Delta t$ -dependent part of the PDF is a convolution of the form

$$T'_i(\Delta t, \sigma_{\Delta t}, S_{\text{tag}}) = \int d\Delta t_{\text{true}} T_i(\Delta t_{\text{true}}, S_{\text{tag}}) \mathcal{R}_i(\Delta t - \Delta t_{\text{true}}, \sigma_{\Delta t}), \quad (12)$$

where  $T$  is the distribution of  $\Delta t_{\text{true}}$ , the true decay time difference, and  $\mathcal{R}$  is a resolution function that parameterizes detector resolution and systematic offsets in the measured positions of vertices.

Taking into account the mistag probability and the effect of tags due to the unreconstructed  $D^0$ , the  $\Delta t_{\text{true}}$  signal PDF in Eq. 12 can be written as

$$T_{\text{sig}} = \frac{1}{4\tau_b} e^{-|\Delta t_{\text{true}}|/\tau_b} \cdot \left\{ 1 - S_{\text{tag}} \Delta\omega(1 - \alpha) + S_{\text{tag}}(1 - 2\omega)(1 - \alpha) \right. \\ \left. \cdot [C \cos(\Delta m_d \Delta t_{\text{true}}) + S \sin(\Delta m_d \Delta t_{\text{true}})] \right\}, \quad (13)$$

where the time-dependent  $CP$  asymmetry parameters  $S$  and  $C$  are the object of the measurement discussed in the present article and  $\alpha$  (see Sec. IV B) is the fraction of events in which the tagging track is from the unreconstructed  $D^0$ . We parameterize possible detector effects leading to a small difference between the mistag probability of  $B^0$  tags ( $\omega^+$ ) and that of  $\bar{B}^0$  tags ( $\omega^-$ ), by using the average mistag rate  $\omega \equiv (\omega^+ + \omega^-)/2$  and the mistag rate difference  $\Delta\omega \equiv \omega^+ - \omega^-$  as parameters of the PDF.

Since the  $B\bar{B}$  combinatorial background is dominated by non- $CP$  final states, the  $CP$  asymmetry is expected to be negligible. However, we allow the PDF to accommodate some contamination from  $CP$  final states. Therefore, we parameterize the  $B\bar{B}$  background  $\Delta t_{\text{true}}$  distribution with a PDF similar to that for signal events given in Eq. 13. We also add a fraction  $f_\delta$  of a  $\delta$ -function, to allow for a zero-lifetime component:

$$T_{\text{comb}} = f_{\text{comb}}^\delta \cdot \delta(|\Delta t_{\text{true}}|) \left( 1 - S_{\text{tag}} \Delta\omega_{\text{comb}}^\delta \right) + \\ + (1 - f_{\text{comb}}^\delta) \cdot \frac{1}{4\tau_{\text{comb}}} e^{-|\Delta t_{\text{true}}|/\tau_{\text{comb}}} \\ \cdot \left\{ 1 - S_{\text{tag}} \Delta\omega_{\text{comb}} + S_{\text{tag}} \cdot \left[ C_{\text{comb}} \cos(\Delta m_d \Delta t_{\text{true}}) + S_{\text{comb}} \sin(\Delta m_d \Delta t_{\text{true}}) \right] \right\}. \quad (14)$$

The second term of the PDF is obtained from Eq. 13 with  $\omega = \alpha = 0$ , as these are not defined for background events. The  $C_{\text{comb}}, S_{\text{comb}}$  parameters describe small fluctuations in the  $\Delta t_{\text{true}}$  distribution of background events and possible  $CP$  event contamination, leading to a small effective  $CP$  violation value.

The  $\Delta\omega$  parameters, which for signal events is the difference in the mistag probabilities for  $B^0$  and  $\bar{B}^0$ , allow for differences in the number of events tagged as a  $B^0$  or  $\bar{B}^0$  in the same background sample. We use this PDF to describe both the  $B^0\bar{B}^0$  and  $B^+B^-$  components.

The PDF for the background due to continuum events is modeled with a simple exponential decay distribution plus a fraction  $f_\delta$  of a  $\delta$ -function:

$$T_{q\bar{q}} = f_{q\bar{q}}^\delta \cdot \left( 1 - S_{\text{tag}} \Delta\omega_{q\bar{q}}^\delta \right) \cdot \delta(|\Delta t_{\text{true}}|) + \\ + (1 - f_{q\bar{q}}^\delta) \cdot \left( 1 - S_{\text{tag}} \Delta\omega_{q\bar{q}} \right) \cdot \frac{1}{4\tau_{q\bar{q}}} e^{-|\Delta t_{\text{true}}|/\tau_{q\bar{q}}} \quad (15)$$

where the parameters  $\Delta\omega_{q\bar{q}}^\delta$  and  $\Delta\omega_{q\bar{q}}$  allow for differences in the number of events tagged as a  $B^0$  or  $\bar{B}^0$  in this sample.

### 3. Resolution Functions

The functions  $T'_i$  of the measured time difference  $\Delta t$ , to be used in the fits, are obtained by convolving the  $T_i$  PDF's of Eq. 13, 14, 15 with the appropriate resolution function for events of type  $i$  ( $i = \text{sig, comb, } q\bar{q}$ ).

The resolution functions are parameterized as the sum of three Gaussian functions:

$$\mathcal{R}_i(t_r, \sigma_{\Delta t}) = f_i^n \mathcal{G}_i^n(t_r, \sigma_{\Delta t}) \\ + (1 - f_i^n - f_i^o) \mathcal{G}_i^w(t_r, \sigma_{\Delta t}) \\ + f_i^o \mathcal{G}_i^o(t_r), \quad (16)$$

where  $t_r = \Delta t - \Delta t_{\text{true}}$  is the residual of the  $\Delta t$  measurement, and  $\mathcal{G}_i^n, \mathcal{G}_i^w$ , and  $\mathcal{G}_i^o$  are the “narrow”, “wide”, and “outlier” Gaussian functions. The narrow and wide Gaussian functions incorporate information from the  $\Delta t$  uncertainty  $\sigma_{\Delta t}$ , and account for systematic offsets in the estimation of  $\sigma_{\Delta t}$  and the  $\Delta t$  measurement. They have the form

$$\mathcal{G}_i^k(t_r, \sigma_{\Delta t}) \equiv \frac{1}{\sqrt{2\pi} s_i^k \sigma_{\Delta t}} \\ \cdot \exp \left( -\frac{(t_r - b_i^k \sigma_{\Delta t})^2}{2(s_i^k \sigma_{\Delta t})^2} \right), \quad (17)$$

where the index  $k$  takes the values  $k = n, w$  for the narrow and wide Gaussian functions, and  $b_i^k$  and  $s_i^k$  are parameters determined by fits. The outlier Gaussian function, describing a small fraction of events with badly measured  $\Delta t$ , has the form

$$\mathcal{G}_i^o(t_r) \equiv \frac{1}{\sqrt{2\pi} s_i^o} \exp \left( -\frac{(t_r - b_i^o)^2}{2(s_i^o)^2} \right). \quad (18)$$

In all fits, the values of  $b_i^o$  and  $s_i^o$  are fixed to 0 ps and 8 ps, respectively, and are later varied to evaluate systematic uncertainties.

## F. Analysis Procedure

After the event selection described in Sec. III B is complete, the rest of the analysis proceeds with a series of unbinned maximum-likelihood fits, performed simultaneously on the on- and off-resonance data samples and independently for the lepton-tagged and kaon-tagged events. The procedure can be logically divided in the following three steps, which we shall discuss in detail in the following paragraphs:

1. In the first step we determine the signal fraction  $f_{\text{sig}}$  in Eq. 4 and the shape of  $\mathcal{M}(m_{\text{rec}})$  and  $\mathcal{F}(F)$  in Eq. 6 for the different classes of events (signal and backgrounds, kaon and lepton tagging categories). This is done by fitting data with the PDF

$$P_i(m_{\text{rec}}, F) = \mathcal{M}_i(m_{\text{rec}}) \mathcal{F}_i(F), \quad (19)$$

ignoring the time dependence; we refer to this step as the kinematic fit.

2. In the second step we determine the tagging dilution due to wrong tag assignments.
3. In the last step we perform the time-dependent fit to the data. We fix all parameter values obtained in the previous steps and use the full PDF of Eq. 6 to determine the parameters of the resolution functions,  $T'_i(\Delta t, \sigma_{\Delta t}, S_{\text{tag}})$ , and the  $CP$  asymmetry values  $C$ ,  $S$  of the signal and of the  $B\bar{B}$  combinatorial background component.

The fitting procedure has been validated using both full Monte Carlo and, where the requested number of events would be too large, the technique of “toy” Monte Carlo. In a toy Monte Carlo, events are described by a small number of variables which are generated according to our PDF’s.

## IV. RESULTS

Event selection yields the numbers of events listed in the top two rows of Table I. The third and fourth rows

TABLE I: Event selection yield. The first uncertainty shown is statistical, while the second uncertainty on the number of continuum events accounts for a 1% relative uncertainty on the on-peak and off-peak luminosities.

|                  | # of events            |                     |
|------------------|------------------------|---------------------|
|                  | kaon tag               | lepton tag          |
| on-peak          | 61179                  | 20855               |
| off-peak         | 1025                   | 51                  |
| continuum        | $9814 \pm 307 \pm 196$ | $488 \pm 68 \pm 10$ |
| $B\bar{B}$       | $51365 \pm 364$        | $20367 \pm 69$      |
| $N_{\text{sig}}$ | $3843 \pm 397$         | $1129 \pm 218$      |

show the number of continuum and  $B\bar{B}$  events calculated, using Eq. 5, from the number of off-peak events in the second row. The numbers of signal events in the last line of the table are calculated using the signal fractions obtained from the kinematic fit described in the next section.

### A. Kinematic Fit

We begin by fitting the shape of our signal,  $\mathcal{M}_{\text{sig}}(m_{\text{rec}})$ , using a large sample of Monte Carlo signal events. The parameters most relevant to determine directly the signal fraction in the data, and consequently our final result for  $S$  and  $C$ , will be released again in the

final kinematic fit. They are (refer to Eq. 8): the Gaussian fraction  $f_G$ , mean value  $m_G$ , and standard deviation  $\sigma_G$ , and are shown in the last section of Table II.

Next we fit the Fisher  $\mathcal{F}_{q\bar{q}}$  and recoil mass  $\mathcal{M}_{q\bar{q}}$  distribution to the off-peak data sample. As the number of off-resonance events selected in the lepton tagged sample is too small to yield convergence, we set the lepton tag sample parameters to the corresponding values obtained from the fit to the kaon tag sample. Due to the small continuum fraction in the lepton sample, we judge that this does not introduce any significant systematic effect. The  $\mathcal{F}_{q\bar{q}}$  parameters are fixed in all subsequent fits.

We initialize the parameters of the  $B\bar{B}$  combinatorial background PDF directly from the data, using a sample of events in which the contribution of signal events is much reduced. We obtain this sample by combining a  $D^*$  with a pion of wrong sign charge (WS sample). We have verified, both on Monte Carlo and in the  $m_{\text{rec}}$  sideband for data, (1.836–1.856 GeV/ $c^2$ ), that the shape of the  $\mathcal{M}(m_{\text{rec}})$  distribution for combinatorial  $B\bar{B}$  background is well described by that of the WS data sample.

To evaluate a possible contribution from a peaking component in the  $B\bar{B}$  background events, we have allowed the Gaussian fraction  $f_G$  in Eq. 8 to float in a fit to a sample of Monte Carlo background events; this fraction is found to be  $0.000 \pm 0.002$ , and is therefore set to zero.

Finally we fit the on-peak data sample, leaving as free parameters the fraction  $f_{\text{sig}}$  of signal events in the  $B\bar{B}$  component, some of the shape parameters of the continuum and  $B\bar{B}$  combinatorial background  $\mathcal{M}_{\text{comb}}$ , some of the signal parameters in  $\mathcal{M}_{\text{sig}}$ , and the shape parameters of the Fisher discriminant  $\mathcal{F}_{B\bar{B}}$ . Table II summarizes the results and provides information about which parameters are released in the fit (statistical uncertainties given) and which ones are taken from previous fits (no uncertainty given).

The final results of the kinematic fits for the kaon and lepton tagged sample are shown in Fig. 3 and Fig. 4.

### B. Determination of mistag probabilities

A common problem of analyses using the partial reconstruction technique is that a fraction of the tracks used in tagging may belong to the unreconstructed  $D^0$ , leading to a mistag of the event. As the tracks originating from the missing  $D^0$  tend to align to its direction of flight, this fraction can be reduced by applying a constraint on the cosine of the CM opening angle  $\theta_{\text{tag}}$  between the tagging track and the direction of the unreconstructed  $D^0$ . We require  $\cos \theta_{\text{tag}} \leq 0.75$  (0.50) for the kaon (lepton) tagged sample.

We find from signal Monte Carlo that before this requirement 26% (13%) of kaon (lepton) tags originate from a missing  $D^0$ . We call these events “ $D$ -tags”, while “ $T$ -tags” are those in which the tagging track (either direct or cascade) is from the tag  $B$ .

TABLE II: Results of the final kinematic fits. The values of fixed parameters are given without uncertainties.

| PDF   | parameter              | description                          | kaon tags                  | lepton tags                |
|---|------------------------|--------------------------------------|----------------------------|----------------------------|
|   | $f_{\text{sig}}$       | Signal fraction                      | $(7.5 \pm 0.7)\%$          | $(5.5 \pm 1.1)\%$          |
| $\mathcal{F}_{B\bar{B}}(F)$                 | $\mu_{B\bar{B}}$       |                                      | $0.723 \pm 0.005$          | $0.721 \pm 0.009$          |
|   | $\sigma_{B\bar{B}}^L$  |                                      | $0.361 \pm 0.003$          | $0.380 \pm 0.006$          |
|   | $\sigma_{B\bar{B}}^R$  |                                      | $0.469 \pm 0.004$          | $0.532 \pm 0.006$          |
| $\mathcal{M}_{q\bar{q}}(m_{\text{rec}})$    | $f^A$                  | Argus fraction                       | 1.0                        | 1.0                        |
|   | $m_{\text{ep}}$        | Argus endpoint ( $\text{GeV}/c^2$ )  | 1.8696                     | 1.8696                     |
|   | $c$                    | Argus exponent                       | $-17 \pm 9$                | -17                        |
|   | $f_{\text{comb}}$      | erf fraction                         | $0.52 \pm 0.15$            | 0.52                       |
|   | $\sigma_{\text{comb}}$ | erf width ( $\text{GeV}/c^2$ )       | $0.0005 \pm 0.0002$        | 0.0005                     |
| $\mathcal{M}_{\text{comb}}(m_{\text{rec}})$ | $f^{\mathcal{A}_1}$    | Argus fraction                       | $0.27 \pm 0.06$            | 1.0                        |
|   | $m_{\text{ep}}$        | Argus end point ( $\text{GeV}/c^2$ ) | 1.8696                     | 1.8695                     |
|   | $c_1$                  | $\mathcal{A}_1$ exponent             | $-49 \pm 38$               | $-15 \pm 2$                |
|   | $c_2$                  | $\mathcal{A}_2$ exponent             | $-0.56 \pm 0.25$           | -                          |
|   | $f_{q\bar{q}}$         | erf fraction                         | $0.26 \pm 0.04$            | $0.41 \pm 0.06$            |
|   | $\sigma_{q\bar{q}}$    | erf width ( $\text{GeV}/c^2$ )       | $(75 \pm 9) \cdot 10^{-5}$ | $(72 \pm 2) \cdot 10^{-5}$ |
| $\mathcal{M}_{\text{sig}}(m_{\text{rec}})$  | $f_G$                  | Gaussian fraction                    | $0.46 \pm 0.06$            | $0.64 \pm 0.12$            |
|   | $m_G$                  | Gaussian peak ( $\text{GeV}/c^2$ )   | $1.8638 \pm 0.0002$        | $1.8635 \pm 0.0003$        |
|   | $\sigma_G$             | Gaussian width ( $\text{GeV}/c^2$ )  | $0.0017 \pm 0.0002$        | $0.0019 \pm 0.0003$        |

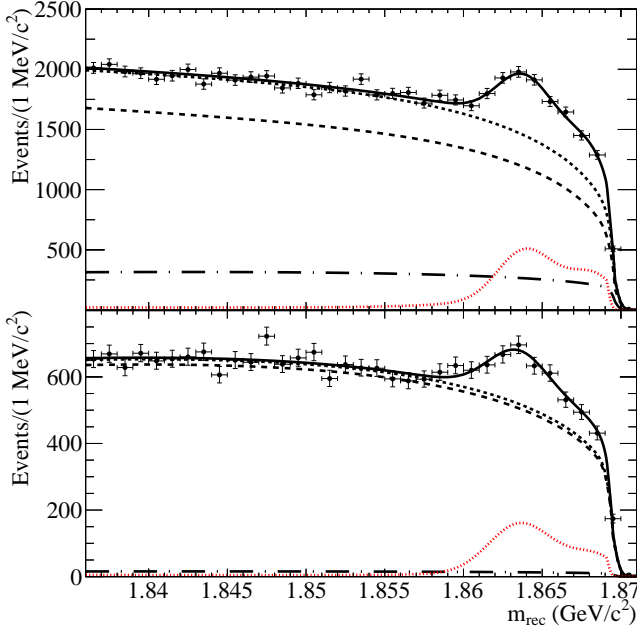


FIG. 3: Result of the kinematical fit of kaon (top) and lepton (bottom) tagged data events, with PDF's overlaid: total PDF (solid line), total background ( $B\bar{B}$  + continuum, short-dashed line),  $B\bar{B}$  combinatorial background (dashed line), continuum  $u, d, s, c$  background (dot-dashed line) and signal (dotted red line).

To reduce dependency on Monte Carlo the fraction  $\alpha$  of  $D$ -tags remaining after the  $\cos \theta_{\text{tag}}$  constraint is measured

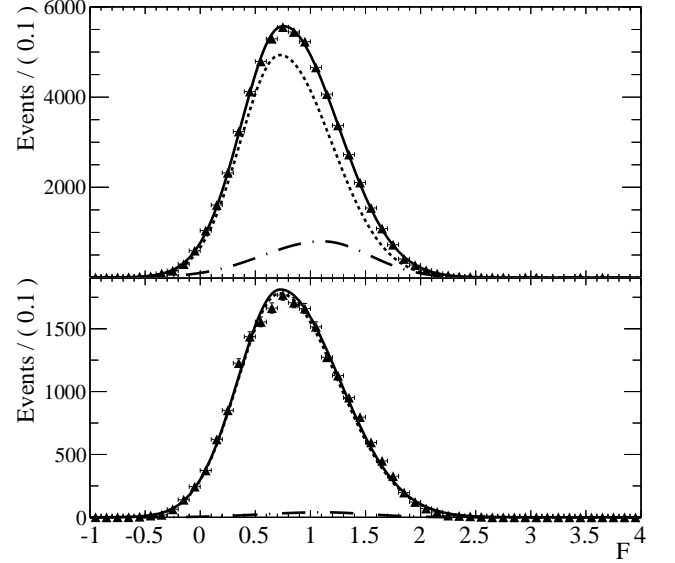


FIG. 4: Result of the kinematical fit of kaon (top) and lepton (bottom) tagged events for the Fisher function, with PDF's overlaid: total  $B\bar{B}$  (solid line),  $B\bar{B}$  (dashed line) and continuum  $u, d, s, c$  background (dash-dotted line).

using data, as explained below.

Defining the total number  $N_T$  ( $N_D$ ) of  $T$  ( $D$ ) tags, the number  $N_T^l$  ( $N_D^l$ ) of them that satisfy the  $\cos \theta_{\text{tag}}$  requirement, and the number  $N_T^g$  ( $N_D^g$ ) of them that do

not,  $\alpha$  is given by:

$$\alpha = N_D^l / (N_D^l + N_T^l) = \frac{f^D p^D}{(f^D p^D + (1 - f^D) p^T)}, \quad (20)$$

where  $p^T = N_T^l / N_T$  ( $p^D = N_D^l / N_D$ ) is the probability, taken from signal Monte Carlo, for a  $T$ -tag ( $D$ -tag) to be from a track satisfying the  $\cos \theta_{\text{tag}}$  cut. The fraction of  $D$ -tags,  $f^D = N_D / (N_T + N_D)$ , is given by

$$f^D = (p^T - f^l) / (p^T - p^D). \quad (21)$$

The fraction  $f^l = N^l / (N^l + N^g)$  is obtained from the kinematic fit of the data:  $N^l$  is the number of signal events that have  $\cos \theta_{\text{tag}} \leq 0.75$  (0.50) and  $N^g$  is the number of signal events with  $\cos \theta_{\text{tag}} \geq 0.75$  (0.50) for kaon (lepton) tag events.

In this way we obtain the values  $\alpha = 0.12 \pm 0.04$  for kaon tags and  $\alpha = 0.00 \pm 0.02$  for lepton tags, as shown in Table III, where we also list the mistag parameters  $\omega$  and  $\Delta\omega$ ,  $\alpha$ ,  $\tau_b$ , and  $\Delta m_d$  that we will need in the final  $\Delta t$  fit.

We use information from signal Monte Carlo events to determine the mistag probability  $\omega = 0.201 \pm 0.002$  ( $0.101 \pm 0.002$ ) and mistag difference  $\Delta\omega = -0.011 \pm 0.003$  ( $0.001 \pm 0.005$ ) for the kaon (lepton) tagged samples. We use the world average value for  $\Delta m_d$  [18], and the values fitted to signal Monte Carlo for  $\tau_b$ , as discussed in Sec. III B.

TABLE III: Values of mistag parameters and  $\alpha$  used in the final fit. The  $b$  lifetime values were obtained from the fit of signal Monte Carlo. The statistical uncertainties are given.

| parameter                  | kaon tags          | lepton tags       |
|----------------------------|--------------------|-------------------|
| $\omega$                   | $0.201 \pm 0.002$  | $0.104 \pm 0.002$ |
| $\Delta\omega$             | $-0.011 \pm 0.003$ | $0.001 \pm 0.005$ |
| $\alpha$                   | $0.12 \pm 0.04$    | $0.0 \pm 0.02$    |
| $\tau_b$ (ps)              | $1.458 \pm 0.014$  | $1.518 \pm 0.018$ |
| $\Delta m_d$ (ps $^{-1}$ ) | $0.507 \pm 0.004$  |                   |

### C. Time Dependent Fit

After the kinematic fit is complete and mistag probabilities are determined, we can proceed to the final  $\Delta t$  fit to extract the  $CP$ -violating parameters  $S$  and  $C$ .

We start by fitting the signal  $\Delta t$  PDF and its resolution function using a pure signal Monte Carlo sample; the parameters determined in this way will be used to initialize the signal PDF, and some of them will be left free again in the final  $\Delta t$  fit.

Next we fit the resolution function parameters and the effective lifetime of the continuum background, using the off-peak data sample. For the kaon tag sample,

the data strongly disfavor a component with nonzero lifetime, therefore we fix  $f_\delta = 1$ , and leave free in the final  $\Delta t$  fit only  $\Delta\omega_\delta$  from Eq. 15. For lepton tags, as the real data sample is too small, we obtain resolution and  $\Delta t$  parameters from continuum Monte Carlo.

We use the continuum parameters obtained above in the next fit stage, where we obtain the  $B\bar{B}$  background resolution function and  $\Delta t$  parameters using real data, by restricting the fit to events in a sideband region ( $1.836$ – $1.856$  GeV/ $c^2$ ) of the  $D^0$  recoil mass distribution. According to Monte Carlo studies the fraction of signal events in this sideband is negligible, and we set it to zero. We fit simultaneously the resolution and lifetime parameters, shown in sections 1 and 3 of Table IV. The fitted values of  $C_{\text{comb}}$  and  $S_{\text{comb}}$  are consistent with 0 as expected.

We are now in a position to perform the final  $\Delta t$  fit, in which we release parameters from the signal, continuum and  $B\bar{B}$  combinatorial background  $\Delta t$  and resolution models, as detailed in Table IV, always with the convention that parameters free (fixed) in the final  $\Delta t$  fit are shown with (without) a fit uncertainty.

The results are also shown in Fig. 5 (6) for the kaon (lepton) tagged samples, where we plot the  $\Delta t$  distributions separately for  $B^0$  and  $\bar{B}^0$  tags, together with the time-dependent raw  $CP$  asymmetry

$$A(\Delta t) = \frac{N_{S_{\text{tag}=1}}(\Delta t) - N_{S_{\text{tag}=-1}}(\Delta t)}{N_{S_{\text{tag}=1}}(\Delta t) + N_{S_{\text{tag}=-1}}(\Delta t)}. \quad (22)$$

For presentation purposes, only data in the restricted signal region  $m_{\text{rec}} > 1.860$  GeV/ $c^2$  are shown in Fig. 5 and Fig. 6, in order to amplify signal/background ratio and be able to see the oscillation. The signal fractions in this region become  $\approx 24\%$  and  $\approx 18\%$  for kaon and lepton tags respectively.

This requirement is not applied to the fit sample, so our numeric results apply to the whole signal region  $m_{\text{rec}} > 1.836$  GeV/ $c^2$ .

## V. SYSTEMATIC UNCERTAINTIES

Our systematic uncertainties on the  $CP$ -violating parameters  $S$  and  $C$  are summarized in Table V. We discuss here the most significant ones.

Most systematic uncertainties in Table V are due to imperfect knowledge of one single parameter fixed in the final  $\Delta t$  fit, having little or no correlation with uncertainties of other parameters. They have been treated by varying them by  $\pm 1\sigma$  and repeating the final  $\Delta t$  fit leaving only the parameters  $S$  and  $C$  free to vary.

Uncertainties in the first two lines have a different character because they are due to parameter sets, in which correlations among parameters belonging to one set are non-trivial. Given the low signal-to-background ratio, correct modelling of the background shape and signal fraction in the kinematic fit is crucial, especially because

TABLE IV: Result of the final full fit. The values of fixed parameters are given without uncertainties.

| PDF                         | parameter                           | description                     | kaon tags          | lepton tags        |
|-----------------------------|-------------------------------------|---------------------------------|--------------------|--------------------|
| $B\bar{B}$ resolution model | $b^n$                               | offset of narrow Gaussian       | $-0.16 \pm 0.01$   | $-0.022 \pm 0.014$ |
|                             | $b^o$                               | offset of outlier Gaussian (ps) | 0.0                | 0.0                |
|                             | $b^w$                               | offset of wide Gaussian         | $-1.0 \pm 0.2$     | $-0.7 \pm 0.7$     |
|                             | $f^n$                               | fraction of narrow Gaussian     | $0.93 \pm 0.01$    | $0.977 \pm 0.004$  |
|                             | $f^o$                               | fraction of outlier Gaussian    | $0.008 \pm 0.001$  | $0.006 \pm 0.002$  |
|                             | $s^n$                               | see eq. 17                      | $1.03 \pm 0.03$    | $1.02 \pm 0.02$    |
|                             | $s^o$                               | see eq. 18 (ps)                 | 8.0                | 8.0                |
|                             | $s^w$                               | see eq. 17                      | 3.0                | 5.6                |
| continuum $\Delta t$        | $\Delta\omega_{q\bar{q}}^\delta$    | see eq. 15                      | $-0.04 \pm 0.02$   | 0.03               |
| $B\bar{B}$ $\Delta t$       | $f_{\text{comb}}^\delta$            | see eq. 14                      | $0.10 \pm 0.02$    | $0.25 \pm 0.02$    |
|                             | $\Delta\omega_{\text{comb}}^\delta$ | see eq. 14                      | $0.04 \pm 0.12$    | $-0.08 \pm 0.07$   |
|                             | $\Delta\omega_{\text{comb}}$        | see eq. 14                      | $-0.025 \pm 0.012$ | $0.012 \pm 0.021$  |
|                             | $\tau_{\text{comb}}$                | effective lifetime (ps)         | $1.318 \pm 0.023$  | $1.272 \pm 0.031$  |
|                             | $C_{\text{comb}}$                   | cosine coefficient              | $-0.022 \pm 0.024$ | $-0.024 \pm 0.041$ |
|                             | $S_{\text{comb}}$                   | sine coefficient                | $0.004 \pm 0.014$  | $-0.023 \pm 0.024$ |
| signal resolution model     | $b^n$                               | offset of narrow Gaussian       | $-0.35 \pm 0.09$   | $-0.3 \pm 0.2$     |
|                             | $b^w$                               | offset of wide Gaussian         | $8 \pm 3$          | –                  |
|                             | $f^n$                               | fraction of narrow Gaussian     | $0.992 \pm 0.007$  | $1.0 \pm 0.1$      |
|                             | $f^o$                               | fraction of outlier Gaussian    | 0.0                | –                  |
|                             | $s^n$                               | see eq. 17                      | $1.13 \pm 0.12$    | $1.17 \pm 0.21$    |
|                             | $s^w$                               | see eq. 17                      | 2.6                | –                  |
| signal $\Delta t$           | $C$                                 |                                 | $+0.117 \pm 0.111$ | $+0.195 \pm 0.147$ |
|                             | $S$                                 |                                 | $-0.417 \pm 0.159$ | $-0.210 \pm 0.200$ |

the  $\mathcal{M}(m_{\text{rec}})$  and  $\mathcal{F}(F)$  PDF's parameters are fixed in the final  $\Delta t$  fit. Consequently, we devised a procedure to evaluate the associated systematic uncertainties, that would also preserve the correlations among parameters belonging to a set.

For each set of parameters in  $\mathcal{M}$  or  $\mathcal{F}$  that become fixed at any stage of our fits, and are not released again in the final  $\Delta t$  fit, a large number  $N_t$  of toy Monte Carlo experiments of the same size as the data are generated and fitted, and the values of parameters in the  $N_t$  experiments are saved. Evaluation of the systematics due to a set of parameters in subsequent fits (in which they become fixed) is made by repeating the latter fits many times over, using the same event sample, but fixing parameters in the set to different values every time, taken from one of the  $N_t$  experiments. In this way, we propagate the variation associated to parameter sets from one fit to the next one, and preserve correct correlations among them. We applied this procedure to obtain the uncertainties in lines 1 and 2 of Table V, which for lepton tagged events are the main source of systematics.

For lepton tags we find that only one Gaussian is sufficient to describe the resolution function ( $f^n = 1$ ). The systematic due to the signal  $s^w$  was evaluated only for kaon tagged events.

Since the mistag parameter  $\omega$  is obtained from Monte Carlo with a very small statistical uncertainty (see Ta-

ble III), we verified the agreement between Monte Carlo and data using a control sample of self-tagging  $B^0 \rightarrow D^{*\mp}\pi^\pm$  events. As a result of this study, we assign a very conservative uncertainty of 15% on  $\omega$ , and evaluate the associated systematic by repeating the final  $\Delta t$  fit varying its central value by  $\pm 15\%$ . This is the largest systematic uncertainty for kaon tagged events.

We estimate the systematic uncertainty associated with fixing the peaking background fraction  $f_G$  in Eq. 8 to zero by setting it to  $\pm 0.002$  for both the kaon and lepton tag samples, repeating the fit, and taking the largest deviation from the value fitted with  $f_G = 0$  as the systematic uncertainty.

The signal  $m_{\text{rec}}$  spectra for the  $CP$ -even and  $CP$ -odd components are different, the latter being slightly harder. This may cause a small acceptance difference of our event reconstruction and selection, leading to a systematic shift in the  $C$  and  $S$  measurement. We have carefully evaluated this effect and found it to be negligible.

As the  $D^{*+}D^{*-}$  final state is a superposition of  $CP$ -even and  $CP$ -odd wave functions, the measured values  $S$  and  $C$  from our data only represent a weighted average of these components, with their inverse squared errors as weights. Since the background shape is not uniform as it goes to zero at the kinematical limit, the weight of the  $CP$ -odd component could be enhanced with respect to the  $CP$ -even one by the lower background level

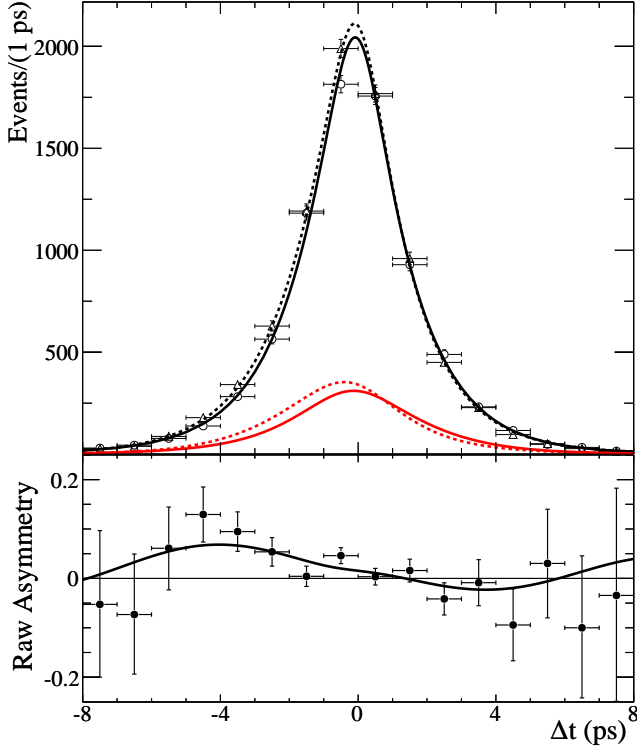


FIG. 5: Top:  $\Delta t$  distribution for  $B^0$  (dashed) and  $\bar{B}^0$  (solid) kaon tags; the lower curves are the corresponding signal PDFs. Bottom: raw time-dependent  $CP$  asymmetry. Only data in the restricted signal region  $m_{\text{rec}} > 1.860 \text{ GeV}/c^2$  are shown.

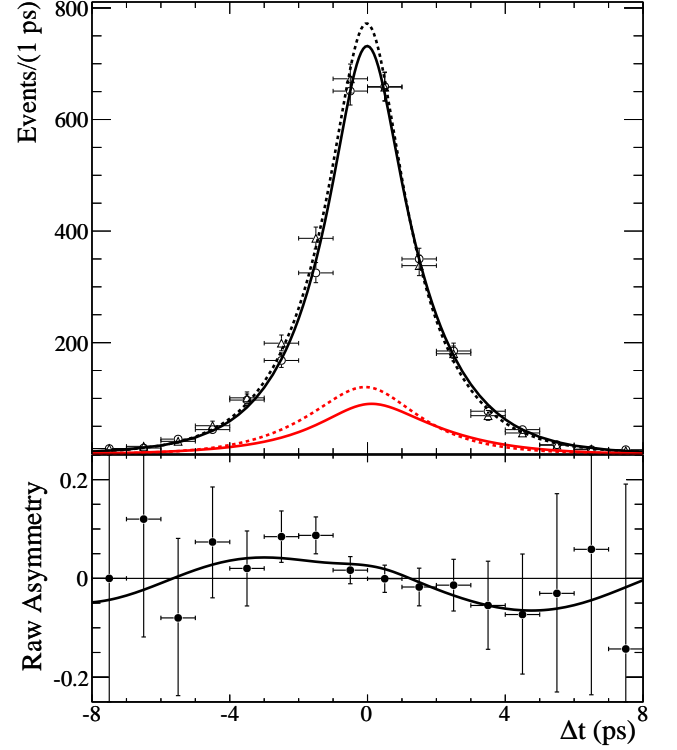


FIG. 6: Top:  $\Delta t$  distribution for  $B^0$  (dashed) and  $\bar{B}^0$  (solid) lepton tags; the lower curves are the corresponding signal PDFs. Bottom: raw time-dependent  $CP$  asymmetry. Only data in the restricted signal region  $m_{\text{rec}} > 1.860 \text{ GeV}/c^2$  are shown.

in the high mass region. To evaluate this effect, we perform  $\Delta t$  fits in the two extreme Monte Carlo configurations, adding to the background sample a pure  $CP$ -odd ( $R_{\perp} = 1$ ) or  $CP$ -even ( $R_{\perp} = 0$ ) sample of signal events, respectively. The number of signal events in both cases is equal to the number of signal events found in data. We find that the differences in the errors of  $S$  and  $C$  are negligible in these two cases and we do not assign a systematic uncertainty to this effect.

As discussed in Sec. IV C,  $\tau_b$  and  $\Delta m_d$  are fixed to the values listed in Table III. We assign the systematic uncertainty due to these assumptions by varying their nominal values of  $\pm 1\sigma$ , and taking half the difference in the fitted values of  $C$  and  $S$  so obtained.

To evaluate bias on  $C$  and  $S$  in our fit, we apply the fit procedure to pure signal Monte Carlo events and compare the results for  $C$  and  $S$  to the generated ones; no significant bias has been observed in either. We therefore quote the statistical uncertainty on these Monte Carlo measurements as the associated systematic uncertainties.

To measure the systematic uncertainty related to imperfect knowledge of the time measurement due to uncertainty in the boost or possible uncorrected misalignment of the SVT, we repeat the time-dependent fit with different sets of realistic misalignments of the SVT and  $\Delta t$

scaling factors. The maximum observed shift with respect to the nominal fit is quoted as the uncertainty.

An important source of systematic uncertainty in our analysis is represented by interference effects from doubly Cabibbo-suppressed decay amplitudes on the tagging side of the event. The non-leptonic  $B$ -meson decays used for tagging are dominated by amplitudes containing a  $b \rightarrow c\bar{u}d$  transition, thus ensuring the correlation of the tagging particle (typically a kaon) with the flavor of the originating  $b$  quark. However,  $\bar{b} \rightarrow \bar{u}cd$  transitions could also contribute, although they are suppressed[22] by a factor  $r' \simeq |(V_{ub}^* V_{cd})/(V_{cb} V_{ud}^*)| = 0.02$ .

As discussed in detail in Ref. [22], this effect cannot be simply reabsorbed into the mistag probability  $\omega$  because the allowed and doubly Cabibbo-suppressed amplitudes can interfere, and thus effectively change the  $\Delta t$  probability density function.

Since our  $\Delta t$  PDF assumes  $r' = 0$  and therefore does not include these effects, the  $C$ ,  $S$  parameters measured by our fit will be different from the observables without tag-side interference by a calculable quantity.

To evaluate the systematic effect in our measurement due to neglecting small terms in the PDF with  $r' \neq 0$ , we follow the prescription in Ref. [22] and perform a simple toy Monte Carlo of  $\delta C \equiv C_{\text{fit}} - C_0$  and  $\delta S \equiv S_{\text{fit}} - S_0$ ,

TABLE V: Systematic uncertainties evaluated for  $C$  and  $S$ . Uncertainties in the top section are independent for kaon and lepton tags, those in the bottom section are correlated.

| Systematic source                    | kaon tags |        | lepton tags |         |
|--------------------------------------|-----------|--------|-------------|---------|
|                                      | $C$       | $S$    | $C$         | $S$     |
| Kinematic fit parameters             | 0.013     | 0.034  | 0.023       | 0.057   |
| Continuum $\Delta t$ fit parameters  | 0.002     | 0.001  | —           | —       |
| Signal $s_w$                         | 0.0002    | 0.0007 | —           | —       |
| $B\bar{B}$ combinatorial $s_w$       | 0.017     | 0.0007 | 0.001       | 0.005   |
| Signal tag side ( $\omega$ )         | 0.012     | 0.045  | 0.002       | 0.002   |
| Mistag difference ( $\Delta\omega$ ) | 0.007     | 0.0004 | 0.007       | 0.0009  |
| Signal $CP$ side ( $\alpha_{D^0}$ )  | 0.006     | 0.017  | 0.002       | 0.002   |
| Peaking background                   | 0.0002    | 0.0003 | 0.0002      | 0.00004 |
| Fit bias (MC statistics)             | 0.011     | 0.018  | 0.012       | 0.019   |
| Tag interference from DCSD           | 0.030     | 0.002  | —           | —       |
| $B^0$ lifetime variation             | 0.0002    | 0.002  | 0.0003      | 0.004   |
| $\Delta m_d$ variation               | 0.0003    | 0.001  | 0.0004      | 0.002   |
| SVT misalignment                     | 0.003     | 0.007  | 0.002       | 0.004   |
| Boost uncertainty                    | 0.002     | 0.006  | 0.005       | 0.007   |
| Total                                | 0.042     | 0.062  | 0.028       | 0.061   |

finding the results reported in Table V. The lepton tags are not affected by this issue.

## VI. PHYSICS RESULTS

The final results for  $C$  and  $S$ , with their correlation coefficient  $\rho$ , including only the statistical uncertainty for kaon and lepton tags, are:

$$\begin{aligned} C &= +0.12 \pm 0.11 \\ S &= -0.42 \pm 0.16 \end{aligned} \quad \rho = 0.0601, \quad \text{kaon tags,}$$

$$\begin{aligned} C &= +0.20 \pm 0.15 \\ S &= -0.21 \pm 0.20 \end{aligned} \quad \rho = 0.0730, \quad \text{lepton tags.}$$

The two samples are statistically independent of each other and can therefore be combined; their statistical uncertainties can be combined in quadrature, but the systematic ones need a more careful treatment.

Indeed, several of the systematic effects listed in Table V are independent for the kaons and lepton tags and are combined in quadrature, while the others are combined taking into account their correlation. Finally we get the combined results of this analysis of

$$\begin{aligned} C &= +0.15 \pm 0.09 \pm 0.04 \\ S &= -0.34 \pm 0.12 \pm 0.05 \end{aligned} \quad \rho = 0.0649.$$

### A. Extraction of $S_+$ and $C_+$

The measured values of  $S$  and  $C$  that we obtain from data only represent a weighted average of the  $CP$  even

and  $CP$  odd wave function components. If penguin amplitudes can be neglected then  $S_+ = -S_-$ ,  $C_+ = -C_-$  and the value of the  $CP$ -even components  $S_+$  and  $C_+$ , which we are interested in, can be obtained using the relations:

$$\begin{aligned} C &= C_+ \\ S &= S_+ (1 - 2R_\perp), \end{aligned}$$

where the factor  $(1 - 2R_\perp)$  represents the dilution introduced by the  $CP$ -odd component  $R_\perp$  in the signal. To compute  $S_+$  we use the value measured by *BABAR* of  $(R_\perp = 0.158 \pm 0.029)$  [8], where the uncertainty is the combined statistical and systematic. To evaluate the related systematic uncertainty, we vary this value by  $\pm 1\sigma$ . We obtain

$$\begin{aligned} C_+ &= +0.15 \pm 0.09 \pm 0.04 \\ S_+ &= -0.49 \pm 0.18 \pm 0.07 \pm 0.04, \end{aligned}$$

where the uncertainties shown are statistical and systematic; the third uncertainty is the contribution from the error on  $R_\perp$  described above.

## VII. SUMMARY

We have measured the time-dependent  $CP$  asymmetry parameters  $C$  and  $S$  in  $B^0 \rightarrow D^{*+} D^{*-}$  decays, from which we have extracted the  $CP$ -even components  $S_+$  and  $C_+$ . This result is an independent determination of the  $CP$ -violating parameters of  $b \rightarrow (c\bar{c})d$  transitions and is compatible with previous measurements from *BABAR* [8] and *Belle* [9] using fully reconstructed decays. It also agrees well with the Standard Model expectation of negligible contributions to the decay amplitude from penguin diagrams and thence with  $S_+ = -\sin 2\beta$ .

## Acknowledgments

We are grateful for the extraordinary contributions of our PEP-II colleagues in achieving the excellent luminosity and machine conditions that have made this work possible. The success of this project also relies critically on the expertise and dedication of the computing organizations that support *BABAR*. The collaborating institutions wish to thank SLAC for its support and the kind hospitality extended to them. This work is supported by the US Department of Energy and National Science Foundation, the Natural Sciences and Engineering Research Council (Canada), the Commissariat à l'Energie Atomique and Institut National de Physique Nucléaire et de Physique des Particules (France), the Bundesministerium für Bildung und Forschung and Deutsche Forschungsgemeinschaft (Germany), the Istituto Nazionale di Fisica Nucleare (Italy), the Foundation for Fundamental Research on Matter (The Netherlands), the Research Council of Norway, the Ministry of Education and Science of the



Russian Federation, Ministerio de Ciencia e Innovación (Spain), and the Science and Technology Facilities Council (United Kingdom). Individuals have received support

from the Marie-Curie IEF program (European Union) and the A. P. Sloan Foundation (USA).

- 
- [1] N. Cabibbo, Phys. Rev. Lett. **10**, 531 (1963).
  - [2] M. Kobayashi and T. Maskawa, Prog. Theor. Phys. **49**, 652 (1973).
  - [3] B. Aubert et al. (BABAR collaboration), Phys. Rev. D **79**, 072009 (2009).
  - [4] K. F. Chen et al. (Belle collaboration), Phys. Rev. Lett. **98**, 031802 (2007).
  - [5] H. Sahoo for the Belle collaboration, e-Print:arXiv:1109.4780[hep-ex].
  - [6] Z. Z. Xing, Phys. Lett. B **443**, 365 (1998).
  - [7] Z. Xing, Phys. Rev. D **61**, 014010 (1999).
  - [8] B. Aubert et al. (BABAR collaboration), Phys. Rev. D **79**, 032002 (2009).
  - [9] B. Vervink et al. (Belle collaboration), Phys. Rev. D **80**, 111104 (2009).
  - [10] Y. Grossman and M. P. Worah, Phys. Lett. B **395**, 241 (1997).
  - [11] M. Gronau, J. L. Rosner and D. Pirjol, Phys. Rev. D **78**, 033011 (2008).
  - [12] R. Zwicky, Phys. Rev. D **77**, 036004 (2008).
  - [13] B. Aubert et al. (BABAR collaboration), Nucl. Instrum. Meth. A **479**, 1 (2002).
  - [14] S. Agostinelli et al. (GEANT4 collaboration), Nucl. Instrum. Meth. A **506**, 250 (2003).
  - [15] D. Lange and A. Ryd, EvtGen: a Monte Carlo Generator for B-Physics, Computing in High Energy Physics 1998, Chicago, Ill.(USA) (1998).
  - [16] W. Menges, IEEE Nuc. Sci. Symp. Conf. Rec. 2005, 3, 1470 (2006).
  - [17] Throughout this article, charge conjugate decay modes are implied.
  - [18] K. Nakamura et al. (Particle Data Group collaboration), J. Phys. G **37**, 075021 (2010).
  - [19] G. Fox and S. Wolfram, Phys. Rev. Lett. **41**, 1581 (1978).
  - [20] R. A. Fisher, Annals of Eugenics **7**, 179 (1936).
  - [21] H. Albrecht (ARGUS collaboration), Phys. Lett. B **340**, 217 (1994).
  - [22] O. Long, M. Baak, R. N. Cahn and D. Kirkby, Phys. Rev. D **68**, 034010 (2003).
  - [23] The Heavy Flavor Averaging Group, “Averages of  $b$ -hadron,  $c$ -hadron, and  $\tau$ -lepton Properties”, arXiv:1010.1589v1 [hep-ex].